**AMOEBOID OLIVINE AGGREGATES IN THE YAMATO-86009 CV3 CHONDRITE.** M. Komatsu[1], T. Fagan[2], M. Miyamoto[3], A.N. Krot[4] and T. Mikouchi[3], [1]The University Museum, University of Tokyo, 7-3-1 Hongo Bunkyo-ku Tokyo, Japan (mutsumi@um.u-tokyo.ac.jp), [2]Department of Earth Sciences, School of Education, Waseda University, 1-6-1 Nishiwaseda Shinjuku-ku Tokyo, Japan, [3]Department of Earth & Planetary Science, University of Tokyo, Japan. [4]Hawaii Institute of Geophysics and Planetology, University of Hawaii at Manoa, USA.

**Introduction:** Amoeboid olivine aggregates (AOAs) are important refractory components of carbonaceous chondrites (except CH and CB chondrites) and have been interpreted to represent solar nebular condensates that experienced high-temperature annealing, but largely escaped melting [1]. Because AOAs in primitive chondrites are composed of fine-grained minerals (forsterite, anorthite, spinel) that are easily modified during postcrystallization alteration, the mineralogy of AOAs can be used as a sensitive indicator of metamorphic or alteration processes [1, 2]. In order to understand the alteration history of the CV3 chondrites, we performed mineralogical studies of AOAs in the Yamato-86009 CV carbonaceous chondrite. Although oxygen isotope compositions of the Y-86009 AOAs have been previously reported [3], their mineralogical studies have not been described yet. Here we report the mineralogy and petrography of AOAs in this meteorite and compare them to those in other CV3 chondrites.

**Samples and analytical procedure:** Two polished thin sections of Y-86009, 51-1 and 51-2, were studied using optical microscopy, SEM, EBSD (Electron back-scattering diffraction) and EPMA.

**Results:** Y-86009 consists of chondrules (53 vol%), AOAs (2 vol%), Ca-Al-rich inclusions (1 vol%) and fine-grained matrix (43 vol%) with isolated mineral fragments (1 vol%). In chondrules, anorthite-normative mesostasis is partly replaced by Al-bearing phyllosilicates. AOAs are commonly surrounded by ~20-μm-thick accretionary rims dominated by fine-grained fayalitic olivine ($Fa_{10-40}$). The rims are often discontinuous and portions of AOAs are observed in direct contact with the Y-86009 matrix. In contrast, fine-grained rims around chondrules are commonly complete.

*Mineralogy and petrography of AOAs*: AOAs are irregularly-shaped objects, 50-750 μm in size, composed of anhedral, fine-grained (1-20 μm) olivines and refractory, Ca-Al-rich nodules. Here we describe three typical AOAs.

AOA #5 is a porous aggregate mainly composed of fine-grained forsteritic olivine ($Fo_{96-99}$) and Al-diopside (Fig. 1). Anorthite is rare; it is largely replaced by fine-grained Mg, Al-silicates, which although are too small to be analyzed by EPMA, appear to be similar in BSE images to phyllosilicates described in the Mokoia CAIs [4]. The anhderal grains of Ca-Fe-rich pyroxene (hedenbergite?) occur along grain boundaries. Euhedral fayalitic olivine grains ($Fa_{63-71}$) overgrow forsterite. Hedenebrgite and fayalite are occasionally observed in direct contact with phyllosilicates.

AOA #2, 170 μm in size, shows similar mineralogy to AOA #5 (Fig. 2). Anorthite is partly replaced by Al-bearing phyllosilicates. Fayalite grains are rather coarse and show inverse compositional zoning, possibly indicating Fe-Mg exchange with a fluid phase.

AOA #15 is a porous aggregate composed of fine-grained olivine ($Fo_{92-99}$), Al-diopside, and spinel (FeO 2-6 wt%). Most of the anorthite is replaced by fine-grained Al-bearing phyllosilicates. Olivine shows enrichment in FeO along the grain boundaries, in contact with phyllosilicates. Some forsterite grains are overgrown by euhedral pyroxene ($Wo_{41}En_{56}Fs_3$, < 10 μm in size) along the rim of the AOA (Fig. 3). This pyroxene has higher content of MnO and $Cr_2O_3$ (~1.9 wt%) than Al-diopside associated with spinel in the interior of the AOA. Secondary fayalitic olivine is absent. In this AOA, an unusual anorthite-like phase (ALP) is observed (Fig. 3). It is ~100 μm in size, and has a homogeneous composition similar to anorthite, but with high FeO (Table 1). EBSD study shows the phase is probably a glass. Porous enstatite ($Wo_7En_{91}$) and a silica-rich phase, which contains minor Mg and Al, are enclosed in the anorthite-like phase.

**Discussion:** AOAs in Y-86009 are mainly composed of forsteritic olivine, Al-diopside and spinel. Although they are texturally similar to those in the reduced and the Allende-like oxidized CV chondrites [7], they show important mineralogical differences. The Y-86009 AOAs experienced hydrous alteration that resulted in replacement of anorthite by phyllosilicates. Most forsterite grains have undergone minimal, if any, alteration; some olivines show enrichment in FeO (Fig. 4). In addition to phyllosilicates, other secondary minerals are fayalite and hedenbergite. These alteration features are similar to those in CAIs, chondrules, and matrices of the Bali-like oxidized CVs [7]. The characteristic alteration minerals of the Allende AOAs, which include zoned ferrous olivine, nepheline and sodalite are absent in the Y-86009 AOAs. We infer that AOAs in Y-86009 were originally similar to those in reduced CVs [9], and subsequently experienced low-temperature aqueous alteration; they largely escaped Fe-alkali metasomatic alteration that resulted in formation of nepheline and sodalite in the Allende AOAs [7]. The presence of the anorthite-like phase (glass?) indicates that some AOAs may have experienced melting and rapid cooling.

**References:** [1] Krot A. N. et al. (2004) *Chem. Erde, 64,* 185-282. [2] Chizmadia L.J. et al. (2002) *MAPS, 37,* 1781-1796. [3] Hiyagon H. and Hashimoto A. (1999) *Science, 283,* 828-831. [4] Cohen R.E. et al. (1983) *GCA, 4I,* 1739–1757. [5] Komatsu M. et al. *MAPS 36,* 629-643 [6] Komatsu M. (2003) Ph.D thesis. University of Tokyo. [7] Krot A.N. et al. (1998)

*MAPS 33,* 623-645. [8] Krot A. N. et al. (1995) *Meteoritics 30,* 748-776.

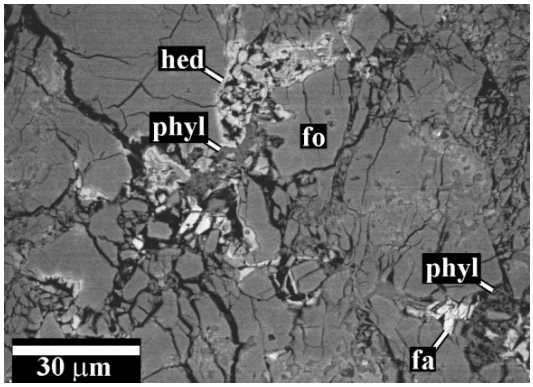


Fig. 1. BSE image of AOA #5 composed of forsteritic olivine (fo) and secondary phyllosilicate (phyl), fayalitic olivine (fa) and hedenbergite (hed).

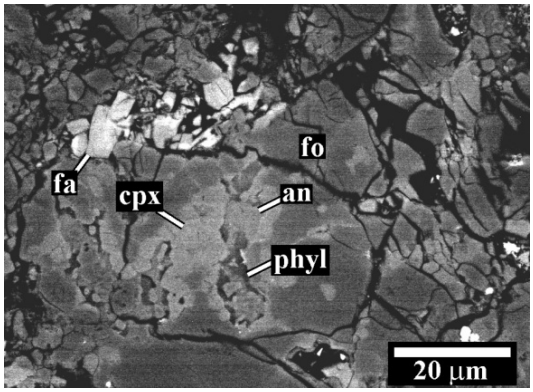


Fig. 2. BSE image of AOA #2 composed of forsteritic olivine (fo), anorthite (an), and Al-diopside (cpx). Anorthite is partly replaced by phyllosilicates (phyl); Forsteritic olivines are overgrown by fayalitic olivine grains (fa) which show inverse compositional zoning.

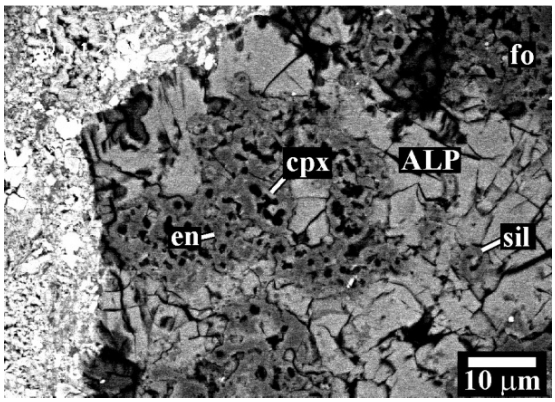


Fig. 3. BSE image of AOA #15 containing anorthite-like phase (ALP) enclosing enstatite (en), Al-diopside (cpx), and silica-rich phase (sil).

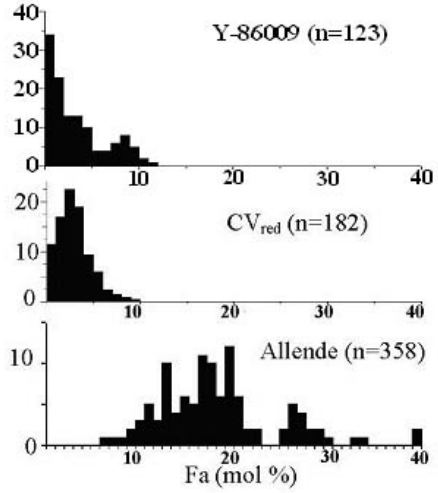


Fig. 4. Histograms of olivine compositions in AOAs from Y-86009, reduced CV chondrites Leoville, Vigarano, Efremovka ($CV_{red}$) [5], and oxidized CV chondrites Allende [6]. Olivines in the Y-86009 AOAs are less ferrous than those from the Allende AOAs and have similar compositional ranges to those from the reduced CV chondrites.

Table 1. Representive analyses of minerals in AOA.

| | fo | cpx | an | en | ALP | rim cpx |
|---|---|---|---|---|---|---|
| AOA # | 15 | 2 | 202 | 15 | 15 | 15 |
| $SiO_2$ | 43.6 | 49.0 | 42.8 | 52.5 | 42.7 | 52.0 |
| $Al_2O_3$ | 0.91 | 5.4 | 37.2 | 5.2 | 33.7 | 5.4 |
| $TiO_2$ | 0.30 | 2.4 | 0.03 | 0.73 | 0.05 | 0.63 |
| FeO | 1.3 | 1.3 | 0.93 | 0.93 | 8.1 | 0.53 |
| MnO | 0.12 | 0.06 | 0.01 | 0.15 | 0.32 | 2.0 |
| MgO | 51.5 | 22.3 | 0.7 | 34.9 | 0.28 | 18.1 |
| CaO | 2.0 | 20.3 | 18.4 | 3.8 | 12.7 | 18.3 |
| $Na_2O$ | 0.05 | n.a. | 0.15 | 0.24 | 2.0 | 0.11 |
| $K_2O$ | 0.04 | n.a. | 0.02 | 0.06 | 0.05 | 0.02 |
| $Cr_2O_3$ | 0.22 | 0.07 | 0.04 | 0.39 | n.a. | 1.9 |
| $V_2O_3$ | 0.03 | n.a. | n.a. | 0.04 | 0.04 | n.a |
| NiO | 0.12 | n.a. | 0.03 | 0.15 | n.a. | 0.03 |
| $P_2O_5$ | n.a. | 0.24 | 0.25 | 0.02 | 0.16 | 0.15 |
| total | 100.2 | 101.0 | 100.5 | 99.1 | 99.9 | 99.0 |
| Fa | 1.4 | - | - | - | - | - |
| Wo | - | 38.8 | - | 7.2 | - | 41.7 |
| En | - | 59.3 | - | 91.4 | - | 57.4 |

an = anorthite; ALP = anorthite-like phase; cpx = Al-diopside; en = enstatite; fo = forsteritic olivine.